ISSN 1330-3651 (Print), ISSN 1848-6339 (Online)
https://doi.org/10.17559/TV-20220221193904
Original scientific paper

Design of Experiment Study of the Parameters that Affect Performance of a Thermoplastic Elastomer Spring of a Hybrid Vehicle Torque Limiter

Cihat GÜL, Ali DURMUŞ*

Abstract: Due to the $C0_2$ emission ratio restrictions, hybrid vehicles become more popular nowadays. Because of that reason, research studies on hybrid vehicles and their powertrain systems have been increased recently. There are several types of hybrid vehicle powertrain structures in use by the car manufacturers; they depend on both the drive modes and the design of conventional and electrical engine layout designed by the car manufacturers. The most known of these structures is the power split hybrid structure. In this study, a thermoplastic elastomer spring was mechanically investigated, which has been designed for torque limiter of a power split type hybrid powertrain. The function of the elastomer spring is to damp the abnormal contact between damper inner metallic components during limiting function. The result of finite element analyses and stiffness measurement result of real parts were compared.

Keywords: hybrid vehicle; isotropic elasticity; multilinear isotropic hardening; nonlinear FEA analysis; thermoplastic elastomer

1 INTRODUCTION

To sustain a clean environment, restrictions over automotive industry become tighter day-by-day. For instance, the EU decided to reduce CO_2 emissions of heavy-duty vehicles by around 60% until 2050. For this purpose, researchers are working on representative simulation tools or methodologies to be able to design new engines accordingly [10]. For passenger cars because of this kind of restrictions, the car manufacturers develop new engine or powertrain structures to reduce fuel consumption and CO_2 emissions. It was declared with European Green Deal report that the target is to reduce reduction of emission by 55% for all cars on the road and for new cars it is to have 0% emission level [1, 2].

Autonomous vehicles are also to have benefits in achieving fuel consumption reduction targets. Tests of autonomous vehicles show that without any efficiency improvement it is possible to gain 3% fuel economy while it can be up to 10% with the efficiency focused control strategies [13].

Only an autonomous drive is not the solution. Excessive improvements to deal with the restrictions is the manufacturing of hybrid vehicles or full electrical vehicles. In comparison with hybrid vehicles, full electrical vehicles are less complex but due to electrical motors capabilities and battery capacities, hybrid vehicles are more popular. Studies show that in the future, electrical vehicles will also play an important role with the improvement of new types of electrical motors [16] and batteries.

With an optimized energy management strategy a hybrid vehicle can save up to 30% - 40% fuel consumption [9]. For this purpose researchers have proposed many energy management methodologies [3, 12, 20]. In these studies, researchers investigated a hybrid powertrain optimization to gain a fuel consumption reduction. In another study researches gained up to 17,5% fuel consumption reduction with a minimization-oriented strategy [11].

Generally, hybrid vehicles are divided into two categories: Hybrid Electric Vehicles (HEV) and Plug-in Hybrid Vehicles (PHEV). The difference between them is the additional charging unit that PHEV vehicles have. From the point of view of the powertrain, there are three different types of hybrid vehicle drive train layouts: series, parallel and power split types (series-parallel) [17]. Their benefits and comparative studies related to energy management strategies have been summarized by Sabri et al.

Hybrid vehicles have a disadvantage too: since they have generally two electric motors, their price is comparatively high. To produce cheaper hybrid powertrains researchers work to develop hybrid powertrains with only one electric motor, which have a limited flexibility with regard to driving modes. Yang et al. have completed a study to develop some driving modes for a hybrid drive line having only a single electric motor [19]. Chen et al. studied on a development of transmission system for parallel hybrid vehicles having a single electric motor [5].

In any case, the studies show that right direction is to use a power split type hybrid powertrain [20], which is the mostly known hybrid powertrain structure. [19]. The first power split type hybrid vehicle is the Toyota Prius in 1997. Ohshima et al. investigated different driving modes of a hybrid vehicle and designed its transaxle. They explained in their studies that inside this type of powertrain structure a torque limiter damper should be used to damp the engine oscillations and to limit the transmitted torque to protect input shaft from excessive vibration torques caused by resonances between the engine and the transaxle [15]. Sasaki S. explained the Toyota Hybrid Powertrain system and its control details. [18]. Further studies completed for the new generation of Toyota Hybrid Sytem are presented by Muta et al. and in these studies a performance increase is gained with the increase of engine and generator revolution amount [14].

1.1 Introduction toTorque Limiter Working Principle

In this study, a design of thermoplastic elastomer spring, which is a component of the torque limiter damper, was developed and investigated. Several geometries were investigated by design of experiments (DOE) methods. In all studies, a commercial thermoplastic elastomer material named Hytrel® 7246 was used.

In hybrid powertrain, the torque limiter has two main functions: 1 - Damping of the engine torque fluctuations and preventing transmission of vibrations to the planet gear set. 2 - Limiting the excessive torque transmission to the input shaft, which is the cause of resonances between the engine and the transaxle.

During normal working conditions, it damps the engine oscillations and prevents the transmission of these vibrations to the planetary gear set. Since the driving modes of the hybrid vehicles contain start-stop situations, resonances between engine and transaxle components can occur. During such resonances, high torque levels can take place. This can be problematic if we consider the fatigue life of the input shaft and drive train components [15]. As mentioned above the function of the torque limiter is to limit transmission of peak torques to the drive train components.

A conventional friction facing slipping which is always under a clamping force between a plate and a cover and is always in the engaged position has provided the limiting function of the torque limiter. It is not slipping below a torque value according to the clamping force. The clamping force on the facing is provided by a belleville type washer, which is in contact with the plate. As mentioned, slipping occurs if the torque value is higher than the slipping torque of the facing which is calculated with the equation below.

$$T_s = n \times \mu \times r \times L \tag{1}$$

T_s is the slipping torque, n is the number of friction surfaces, μ is friction coefficient of the facing material, L is the load provided by Belleville washer rand r is the mean radius of friction surface in the above formula.

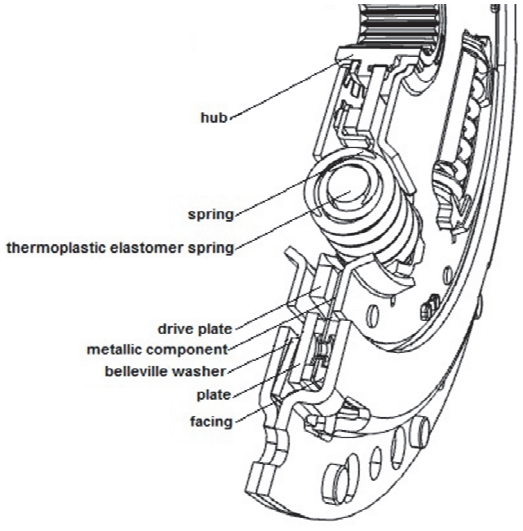

Figure 1 Schematic view of torque limiter-damper

Until the slipping starts, the torque provided by engine is transmitted to the damper components by the facings. The facings have been assembled to the damper by a metallic component. With the help of that metallic component, torque transmission is provided to the input shaft through springs. Accordingly, springs compression occurs on the damper side. Compression of the springs is provided with the retainer plates. One of them is assembled to the metallic component and the other one is assembled to the first one with a stop pin. Schematic view of the system is given in Fig. 1.

With the rotation of the retainer plates, the spring compression starts and the damping can be done with this compression-decompression. However, after a defined torque level, the compression stops and the drive plate, which takes the torque from the springs and transmits it to the hub, is starting to contact the stop pin. This metallic contact is not a preferred contact in a hybrid vehicle transmission; it produces an abnormal noise and will disturb the driver. Because of that reason before the contact occurs, an intermediate stiffness phase is designed to provide a smooth contact between the drive plate and the stop pin. This new stiffness phase is provided by thermoplastic elastomer springs, which are working as compression springs as sketched in Fig. 2.

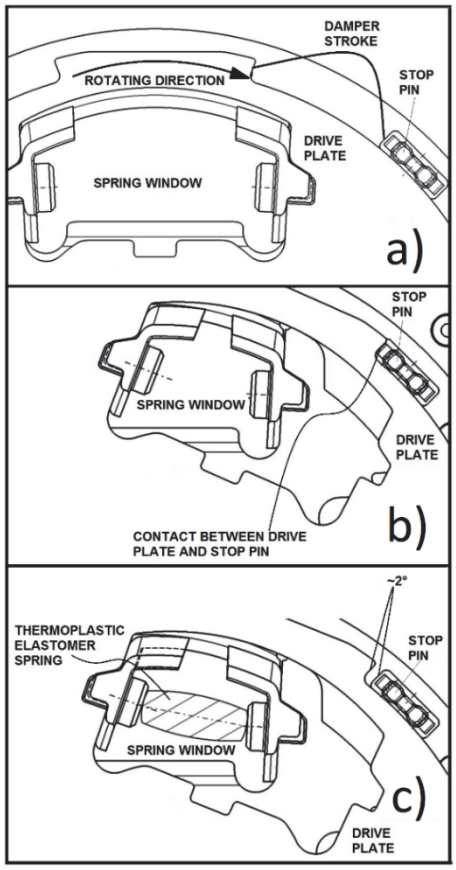

Figure 2 Schematic view drive plate-stop pin contact; a) Initial position of drive plate; b) Damper full stroke with no thermoplastic elastomer spring/drive plate in contact with stop pin; c) Damper stroke with thermoplastic elastomer spring /~2° left to contact of drive plate and stop pin

They are starting to compress at the end of the damper with usually ~1° to 2° stroke.

During the normal operating conditions of the damper side of the torque limiter, no compression of the elastomer spring takes place. But if there is a resonance due to the high torque production before the slippage of the torque limiter, the elastomer springs start to compress till the end of the damper stroke and then slipping of the torque limiter will start. Usual damper curve with its phases are plotted in Fig. 3.

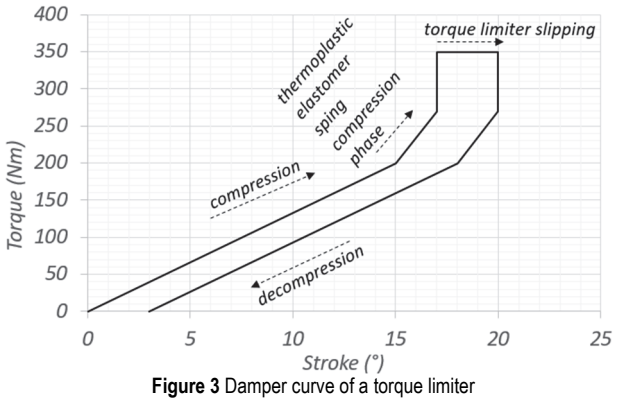

Figure 3 Damper curve of a torque limiter

2 DESIGN FOR EXPERIMENT

As mentioned in the previous section at this type of a damper design, thermoplastic elastomer springs are working inside the main damper springs. Their design is dependent on the inner geometry of spring. However, at the same time they need to provide the required stiffness during their compression. In this study, the stiffness in the compression phase of the thermoplastic elastomer spring was chosen as 70Nm/°. Moreover, with the calculation given below, the required stiffness of thermoplastic elastomer spring has been calculated:

$$S_2 = S_1 + \frac{k_{es} \cdot 2 \cdot \pi \cdot r}{360} \cdot r \cdot n_{es} \tag{2}$$

S_1 = stiffness value of damper springs (Nmm/°),
S_2 = stiffness value of damper springs with elastomer spring (Nmm/°),
k_{es} = stiffness value of elastomer spring (N/mm),
r = application radius of the spring windows,
n_{es} = number of elastomer spring.

In order to achieve the above stiffness value coming from the thermoplastic elastomer spring, a base design was defined as shown in Fig. 4.

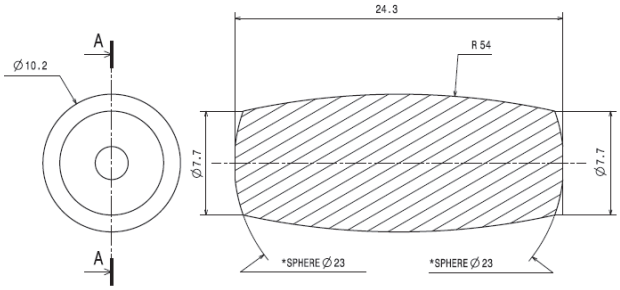

Figure 4 Thermoplastic elastomer spring base design

As mentioned earlier the target stiffness of the thermoplastic elastomer spring is 7 0Nm/°. In addition to this target, the design has to provide loss of height, which has to be as little as possible, with the loads acting on thermoplastic elastomer spring. In that study, different geometrical investigations were done. DOE studies were carried out to see the effect of the geometry to both the stiffness and the loss of length.

Geometries to be investigated in that study are sketched in Fig. 5.

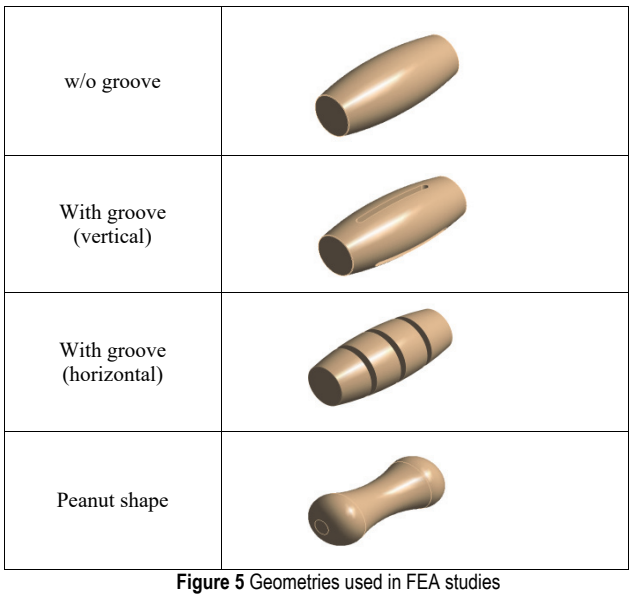

Figure 5 Geometries used in FEA studies

3 EXPERIMENTAL STUDIES

3.1 Finite Element Analysis Model

The finite element analyses were completed using the software Ansys Workbench with the geometries defined above and the material Hytrel 7246. Hytrel 7246 is a thermoplastic elastomer produced by DuPont™. The mechanical behaviour and thermal conductivity value are taken from specification handbook (Hytrel Design Guide) and the mechanical behaviour of material is plotted in Fig 6.

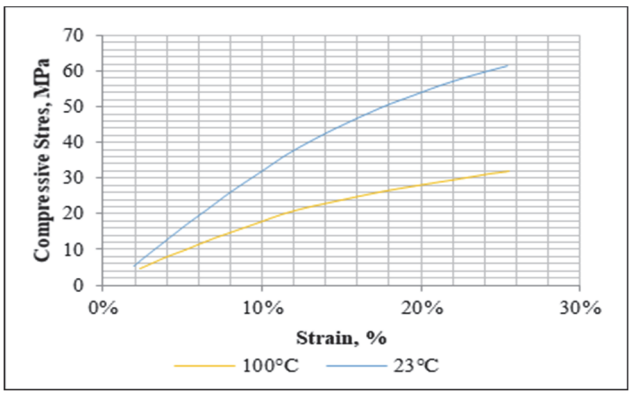

Figure 6 Stress-strain data of Hytrel 7246 material

The material data in Fig. 6 provided by the raw material manufacturer is the engineering stress as the function of engineering strain. In order to use that data in the FEA calculation a transformation to true stress as function of true strain has to be done [6].

$$\sigma_t = \sigma_e \left(1 + \varepsilon_e\right) \tag{3}$$

In the above formula, σ_t is the Cauchy or true stress. The Henky or true strain ε_t is calculated with the formula below:

$$\varepsilon_t = \mathrm{Ln}\left(1 + \varepsilon_e\right) \tag{4}$$

Using these formulas, the transformation to true stress and strain was done for the material data at 23 °C. It can be seen in Fig 7.

Based on true stress / true strain data elastic modulus of the material is calculated as 395 MPa. This input was used in Anysys workbench in combination with an isotropic elasticity model and a Poisson's ratio of 0.4.

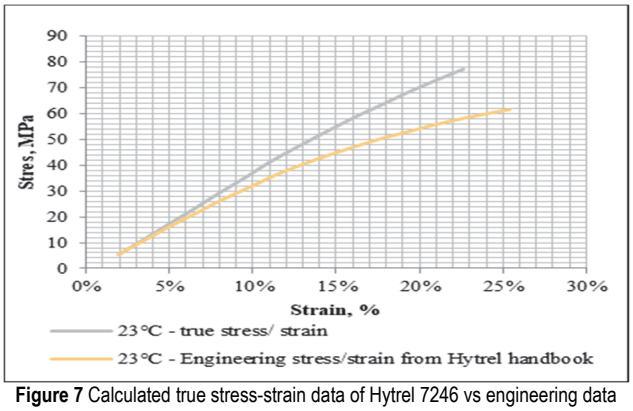

Figure 7 Calculated true stress-strain data of Hytrel 7246 vs engineering data

Nevertheless, the above input data are not sufficient to consider plastic deformation of the thermoplastic elastomer spring under compression, which is one of the key targets of the study. In order to achieve this, the multilinear isotropic hardening material model is applied in Ansys Workbench. That property requirement is plastic strain level of the material. It is calculated with the following formula:

$$\varepsilon_p = \varepsilon_e - \left(\frac{\sigma_e}{E}\right) \tag{5}$$

The plastic stress strain data calculated with the above formula can be seen in Fig. 8.

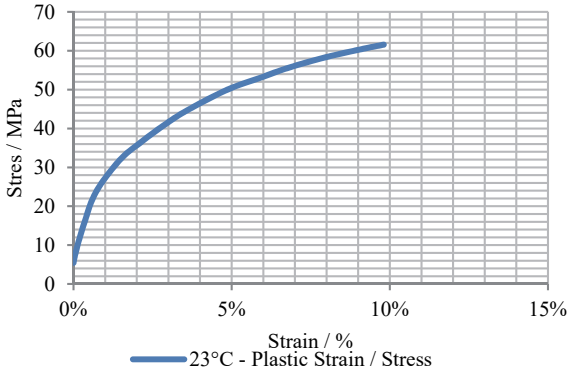

Figure 8 Calculated plastic stress-strain data of Hytrel 7246

The boundary conditions are modelled as shown in Fig. 9. In addition to these boundary conditions steady state thermal input is entered with thermal conductivity property of material which is 0,22 W/m°K [6]. Initial temperature is taken as 23 °C and it is kept constant during loading state which is same as the tests completed at laboratory.

Contact between the planes and elastomer spring is defined as frictional contact with the friction coefficient 0,1. Augmented Lagrange formulation has been used for the contact definition. Meshing of the elements completed with quadrilateral elements. With the sizing option at notch sections or at limit areas sizing quality is increased.

For the all investigated geometries, the same FEA methodology has been followed up. The thermoplastic elastomer springs were compressed between the plates just until a 2 mm compression occurs. Then their stiffness graphs, stress values and permanent deformation values have been recorded.

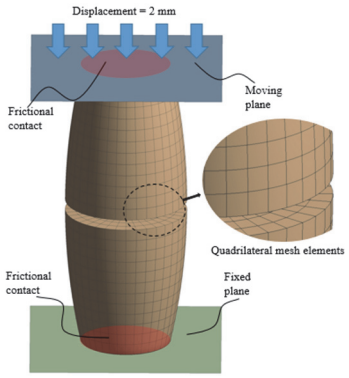

Figure 9 Boundary conditions

3.2 Measurements and Correlation

An initial FEA study is completed with the base design (without grooves). In parallel, this geometry was produced with a prototype tooling and experimentally investigated using a Zwick Roell universal compression testing machine.

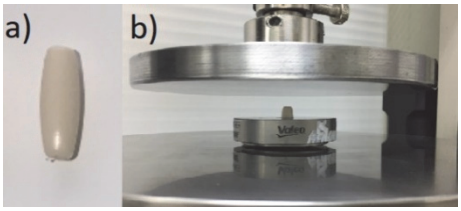

Figure 10 Real part measurements; a) Prototype part; b) Zwick roell testing machine adaptation

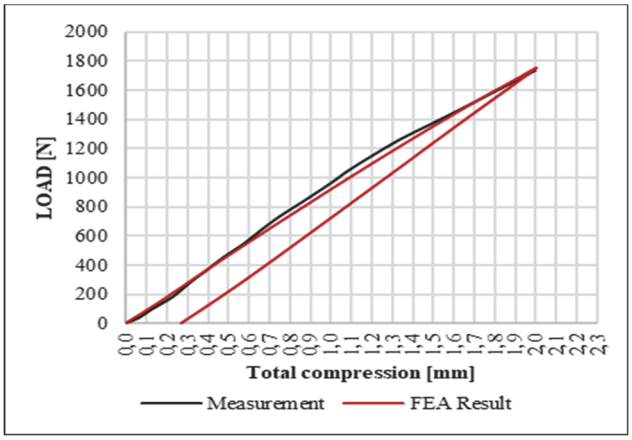

Figure 11 FE analysis result comparison with measurement of real part

In Fig. 11, the measurement data of the thermoplastic elastomer spring is compared with the load vs. stroke data from the FEA calculation.

Another output of the same study is the comparison of the length loss of the thermoplastic elastomer spring. This value loss of length is an excessive output and the target, which is to reduce it as much as possible. If it is too high,

thermoplastic elastomer spring will not be compressed to its designed value during the following actuation. In Tab. 2 measurements results that have been completed for different test speeds can be seen.

Table 1 Loss of length under different test speeds

Test speed	Sample	Loss length / mm
10 mm/min	1	0,27
	2	0,28
	3	0,26
20 mm/min	1	0,27
	2	0,26
	3	0,26
Average		0,67

As seen in the above table, the speed has no significant effect on the loss of length of the spring. The loss of length value is also an output of the FEA studies. Fig. 12 is showing the loss of length simulated by FEA calculations by changing the parameter *R*. In the same figure, the measurement result is indicated to show the correlation between FEA result and the experiment.

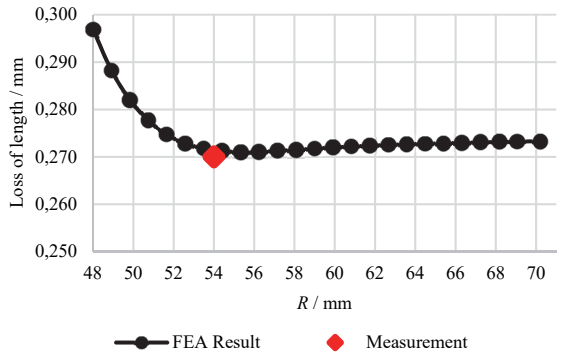

Figure 12 Calculated change of loss of length by "*R*" parameter

A similar graph was gained for load change by parameter "*R*", which is shown in Fig. 13.

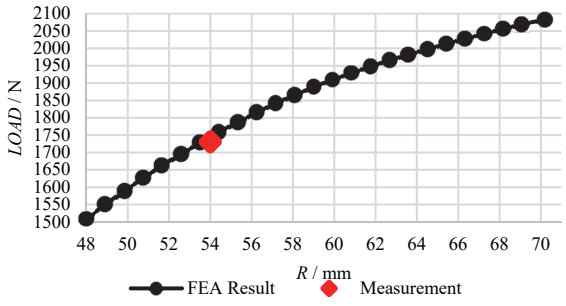

Figure 13 Calculated change of load by "*R*" parameter

3.3 Design of Experiments (DOE) Studies

With the above FEA studies a well correlated model was proved. Based on this model a DOE study was completed to the base design to understand the effects of each geometrical parameter to both the load and the loss length characteristics. The dimensional parameters used in DOE study are as in Fig. 14 and in Tab. 2.

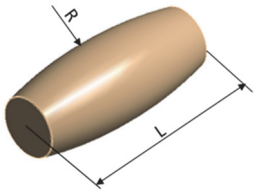

Figure 14 DOE parameters of base design

Table 2 Parameter table of base design

Parameter	Minimum	Maximum
Length, *L* / mm	22,3	28,3
Outer Radius, *R* / mm	48	70

The result of the DOE study with the above parameters is visualized as in Fig. 15. With the decrease of the outer radius of the geometry loss of length is increasing which means that plastic deformations on material are increasing. The lowest loss length value is found with maximum outer radius and when length is maximum too.

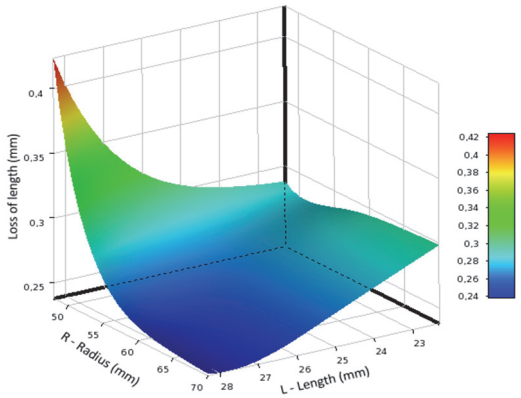

Figure 15 Result of DOE study of base design

The following studies are completed with the same methodology to investigate the effect of different geometries on the loss of length.

The parameters of the peanut shape geometry used in the DOE study are shown in Fig. 16.

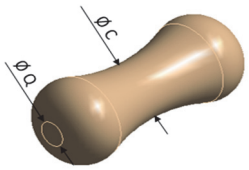

Figure 16 DOE parameters of peanut shape design

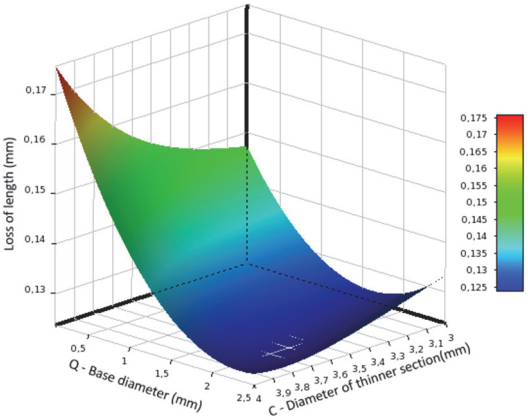

Figure 17 Result of DOE study of peanut shape design

Table 3 Parameter table of peanut design

Parameter	Minimum	Maximum
Inner diameter, ø*C* / mm	3	4
Base diameter, ø*Q* / mm	0,1	2,5

The result gained with the DOE study of the peanut shape is shown in Fig. 17.

The parameters of design with the horizontal grooves used in the DOE study are visualized in Fig. 18.

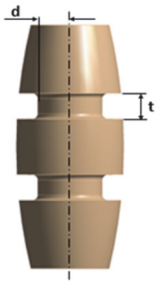

Figure 18 DOE parameters of design have horizontal grooves

Table 4 Parameter table of design have horizontal grooves

Parameter	Minimum	Maximum
Groove diameter, *d* / mm	1	2,5
Groove width, *t* / mm	0,8	2,2
Groove quantity	1	2

The results gained with DOE study of the design with horizontal grooves are shown below in Fig. 19 and Fig. 20.

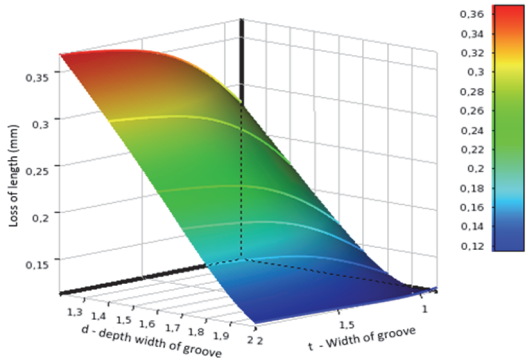

Figure 19 Result of DOE study of design has 1 horizontal groove

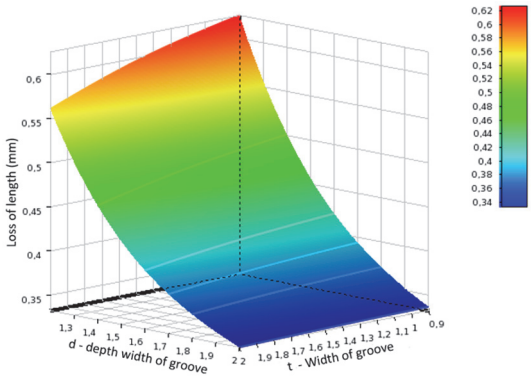

Figure 20 Result of DOE study of design has 2 horizontal grooves

The parameters of design with the vertical grooves used in its DOE study is shown in Fig. 21.

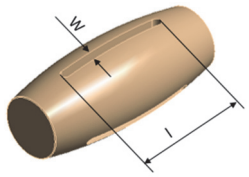

Figure 21 DOE parameters of design have vertical grooves

Table 5 Parameters table of design have vertical grooves

Parameter	Minimum	Maximum
Groove diameter, *w* / mm	1	2.5
Groove length, *l* / mm	10	16
Groove quantity	2	3

The effects of the above parameters to the outputs are visualised in Fig. 22 and Fig. 23.

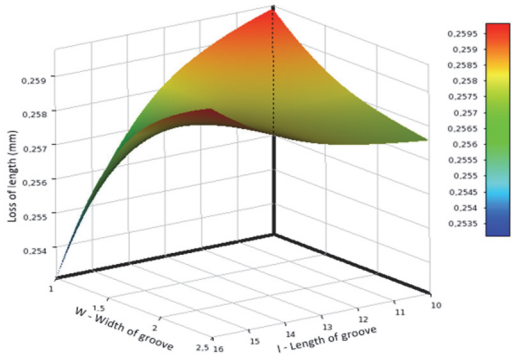

Figure 22 Result of DOE study of design has 2 vertical grooves

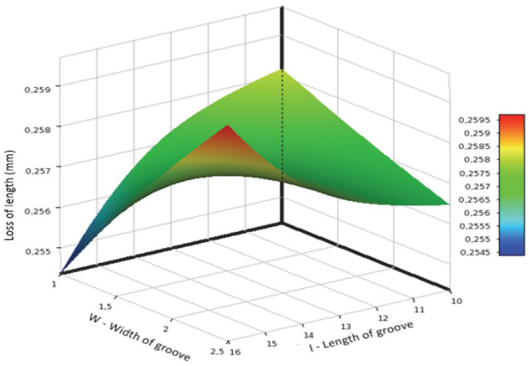

Figure 23 Result of DOE study of design has 3 vertical grooves

As seen in the above results, the design with horizontal grooves has the higher variation and is the best design to sustain a less loss of length. The graph of the load vs. the loss of length of each design is shown in Fig. 24.

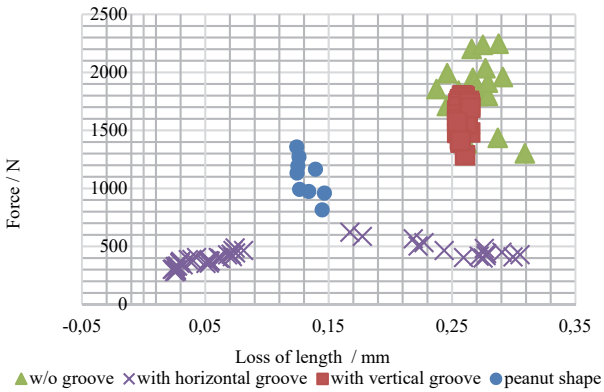

Figure 24 Comparative graph of the load x vs. the loss of length of each design

The final step of the investigation is to define the design rules to the geometry giving the best performance, which is the design with the horizontal grooves. To conclude, a new DOE study is initiated with the parameters given below in Fig. 25 and Tab. 6.

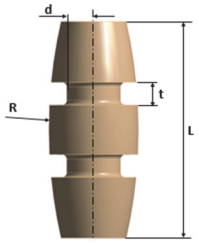

Figure 25 Design parameters of geometry used in DOE study have horizontal grooves

Table 6 Design parameters have horizontal grooves

Parameter	Minimum	Maximum
Groove diameter, d / mm	0,5	3
Groove width, t / mm	0,5	3
Spring length, L / mm	24	30
Outer radius, R / mm	48	70
Groove quantity	1	3

With the above design parameters, a DOE study was completed and design rules were created for the thermoplastic elastomer spring. The results are given in the results section.

4 RESULTS & DISCUSSIONS

At the end of the DOE study with the parameters in Tab. 6 design rules were created:

Rule 1: $2L \leq R \leq 3L$.

This rule is explaining how "R" has to be chosen at design phase to gain a minimum loss of length. DOE result of that rule is as in Fig. 26.

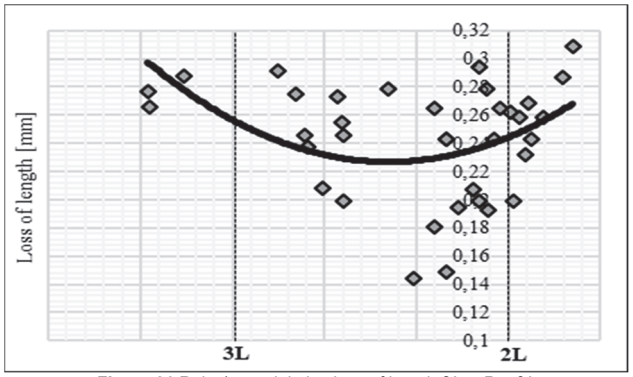

Figure 26 Rule 1: to minimize loss of length $2L \leq R \leq 3L$

Rule 2: total $t(n \times t) \geq$ compression amount.

Rule 2 is explaining design criteria for the total groove width to get a minimum loss of length.

Rule 3: $n \times d \geq$ compression amount.

Rule 3 is explaining the design criteria for the depth of the groove to minimize loss of length.

The first three rules are defined to minimize the loss of length of the thermoplastic elastomer spring under compression. The following two rules are defined to characterize the functional curve of the torque limiter damper.

Rule 4: If total $t(n \times t) \geq$ compression amount, the thermoplastic elastomer spring will provide a single slope curve at the torque limiter damper functional curve as shown in Fig. 29.

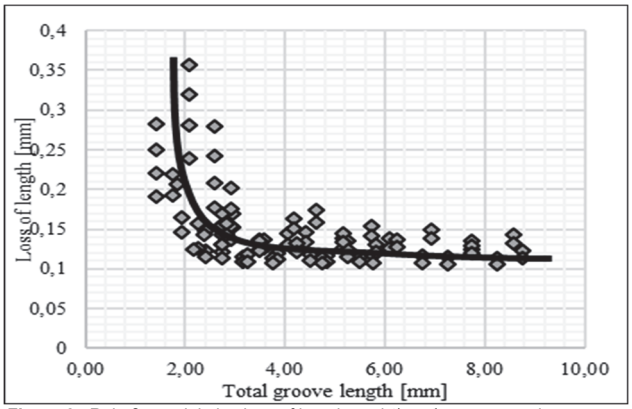

Figure 27 Rule 2: to minimize loss of length total $t(n \times t) \geq$ compression amount

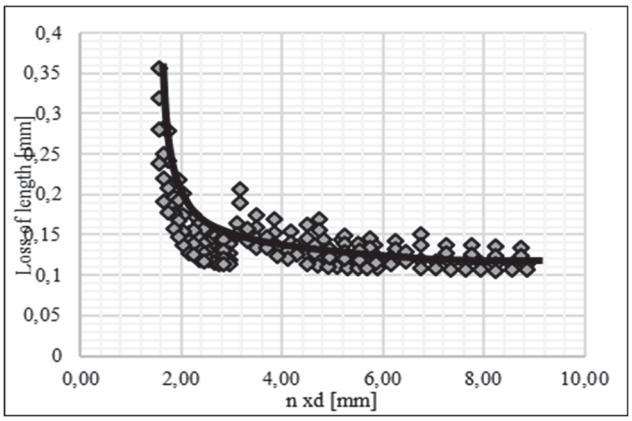

Figure 28 Rule 3: to minimize loss of length n x $d \geq$ compression amount

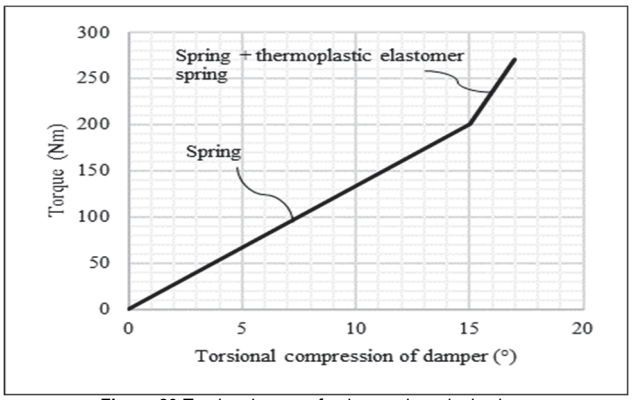

Figure 29 Torsional curve of a damper has single slope

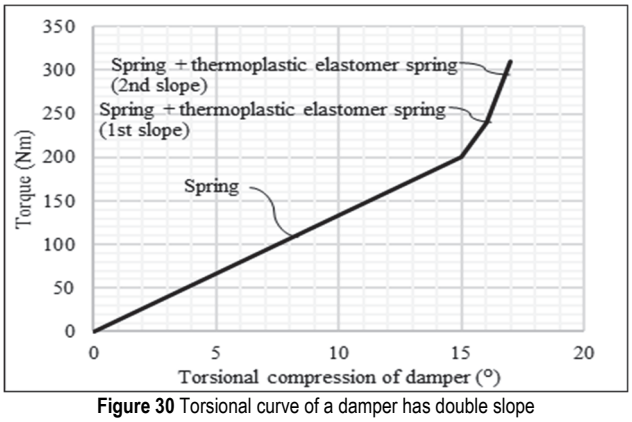

Figure 30 Torsional curve of a damper has double slope

Rule 5: If total $t(n \times t)$ < compression amount, the thermoplastic elastomer spring will provide a double slope curve at torque limiter damper functional curve as shown in Fig. 30.

5 CONCLUSION

Based on different DOE studies, the effect of geometrical parameters to the load and loss of length characteristics of thermoplastic elastomer springs were shown. Design constraints and rules were created to one of them. This analysis study will be a starting point to continue with different material properties and parametrical geometries. Conclusion can be done as below:
- Thanks to horizontal groove and dimensional changes, a large variation of load requirements can be answered.
- Increase of the parameter *R* implies decrease of the amount of loss of length.
- The peanut shape has no excessive benefit on the loss of length.
- The width of the groove does not influence the loss of length behaviour of the design having horizontal grooves.
- The depth of the groove has an excessive effect on the loss of length behaviour of the design having horizontal grooves.
- 3 rules were created for the design having horizontal grooves to minimize the loss of length.
- 2 rules were created to define how to design groove geometry for the required damper slope type.

6 REFERENCES

[1] https://ec.europa.eu/info/strategy/priorities-2019-2024/european-gree-deal/transport-and-green-deal_en

[2] https://ec.europa.eu/info/strategy/priorities-2019-2024/european-green deal/delivering-european-green-deal_en

[3] Aghaei, J., Nezhad, A. E., Rabiee, A., & Rahimi, E. (2016). Contribution of Plug in Hybrid Electric Vehicles in power system uncertainty management. *Renewable and Sustainable Energy Reviews*, *59*(2016), 450-458. https://doi.org/10.1016/j.rser.2015.12.207

[4] Arriaga, A., Lazkano, J. M., Pagaldai, R., Zaldua, A. M., Hernandez, R., Atxurra, R., & Chrysostomou, A. (2007). Finite-element analysis of quasi-static characterization tests in thermoplastic materials: Experimental and numerical analysis results correlation with ANSYS. *Polymer Testing*, 26(2007), 284-305. https://doi.org/10.1016/j.polymertesting.2006.10.012

[5] Chen P. T., Pai P. H., Yang C. J., & Huang K. D. (2019). Development of Transmission Systems for Parallel Hybrid Electric Vehicles. *Applied Sciences*, *9*. https://doi.org/10.3390/app9081538

[6] Dean, G. & Mera, R. (2004). Determination of Material Properties and Parameters Required for the Simulation of Impact Performance of Plastics Using Finite Element Analysis. *NPL Report,* DEPC-MPR 007.

[7] Dupont (2013). *Hytrel Design Guide.*

[8] Ehsani, M., Gao, Y., & Butler, K. L. (1999). Application of Electrically Peaking Hybrid (ELPH) Propulsion System to a Full-Size Passenger Car Simulated Design Verification. *IEEE Transaction on Vehicular Technology*, *48*(6), 1779-1787. https://doi.org/10.1109/25.806770

[9] Emadi, A., Rajashekara, K., Williamson, S. S., & Lukic, S. M. (2005). Topological Overview of Hybrid Electric and Fuel Cell Vehicular Power System Architectures and Configurations. *IEEE Trans. On Vehic. Technol., 54*(3), 763-770. https://doi.org/10.1109/TVT.2005.847445

[10] Fontaras, G., Grigoratos, T., Savvidis, D., Anagnostopoulos, K., Luz, R., Rexeis, M. & Hausberger, S. (2016). An experimental evaluation of the methodology proposed for the monitoring and certification of CO2 emissions from heavy duty vehicles in Europe. *Energy*, *102*(2016), 354-364. https://doi.org/10.1016/j.energy.2016.02.076

[11] García, A., Carlucci, P., Monsalve-Serrano, J., Valletta, A. & Martínez-Boggio, S. (2021). Energy management optimization for a power-split hybrid in a dual-mode RCCI-CDC engine. *Applied Energy*, *302*. https://doi.org/10.1016/j.apenergy.2021.117525

[12] Ibrahim, M., Jemei, S., Wimmer, G., & Hissel, D. (2016). Nonlinear autoregressive neural network in an energy management strategy for battery/ultra capacitor hybrid electrical vehicles. *Electric Power Systems Research*, *136*(2016), 262-269. https://doi.org/10.1016/j.epsr.2016.03.005

[13] Mersky, A. C. & Samaras, C. (2016). Fuel economy testing of autonomous vehicles. *Transportation Research Part C*, *65*(2016), 31-48. https://doi.org/10.1016/j.trc.2016.01.001

[14] Muta, K., Yamazaki, M., & Tokieda, J. (2004). Development of New-Generation Hybrid System THS II-Drastic Improvement of Power Performance and Fuel Economy. *Journal of Engines, SAE Transactions*, *113*(*3*), 182-192. https://doi.org/10.4271/2004-01-0064

[15] Ohshima, K., Kondo, K., Ibaraki, R., & Matsui, H. (1999). Development of transaxle for hybrid vehicle. *JSAE Review*, *21*(2000), 343-347. https://doi.org/10.1016/S0389-4304(00)00047-3

[16] Riba, J., Lopez-Torres, C., Romeral, K., & Garcia, A. (2016). Rare-earth free propulsion motors for electric vehicles: A technology review. *Renewable and Sustainable Energy Reviews*, *57*(2016), 367-379. https://doi.org/10.1016/j.rser.2015.12.121

[17] Sabri, M., Danaplasingam, K. A., & Rahmat, M. F. (2016). A review on hybrid electric vehicles architecture and energy management strategies. *Renewable and Sustainable Energy Reviews*, *53*(2016), 1433-1442. https://doi.org/10.1016/j.rser.2015.09.036

[18] Sasaki, S. (1998). Toyota's Newly Developed Hybrid Powertrain. *International Symposium on Power Semiconductor Devices & ICs, Kyoto,* 17-22. https://doi.org/10.1109/ISPSD.1998.702540

[19] Yang, Y., Hu, X., Pei, H., & Peng, Z. (2016). Comparison of power split and parallel hybrid powertrain architectures with a single electric machine : Dynamic programming approach. *Applied Energy*, *168*(2016), 683-690. https://doi.org/10.1016/j.apenergy.2016.02.023

[20] Zulkefli, M., Zheng, J., Sun, Z., & Liu, H. X. (2014). Hybrid powertrain optimization with trajectory prediction based on inter vehicle communication and vehicle infrastructure integration. *Transportation Research Part C*, *45*(2014), 41-63. https://doi.org/10.1016/j.trc.2014.04.011

Contact information:

Cihat GÜL, PhD Student
Research & Development Department,
Valeo Otomotiv San.ve Tic. A.Ş, Demirtas Dumlupinar OSB Mh. Istanbul Cd.
No: 614 Bursa ,16245, Turkey
E-mail: cihat.gul@valeo.com

Ali DURMUŞ, PhD Prof.
(Corresponding author)
Department of Mechanical Engineering,
Bursa Uludağ University,
Bursa, 16059, Turkey
E-mail: adurmus@uludag.edu.tr